Solving Boltzmann Equation for Coscattering DM

Xucheng Gan

Our goal is to solving the relativistic non-integrable Boltzmann equation in early universe(FLRW metric) numerically. Firstly, we shall try to solve Integrable Boltzmann equation and then in later research we can try more complicated non-integrable Boltzmann equation.

1 Introduction

Boltzmann equation has important application in cosmology. Let's numerically solve it. Integrable version firstly and in the future non-integrable version. Necessary analysis and self-consistency check is discussed. :)

2 Formulas in cosmology

The Planck mass

$$M_{pl} = \sqrt{\frac{\hbar c}{8\pi G}} \tag{1}$$

Here(Also in the later calculation) we choose $\hbar = 1$, $c = 1$. So we have

$$8\pi G = \frac{1}{{M_{pl}}^2} \tag{2}$$

Entropy is conserved

$$Sa^3 = const \tag{3}$$

$$(or) \quad S(x) = \frac{S_0}{x^3} \tag{4}$$

$$(or) \quad \frac{dS}{dt} + 3HS = 0 \tag{5}$$

1st Friedmann equation is(From [1] [7] [9])

$$H^2 = \frac{8\pi G}{3}\rho - \frac{k}{a} \tag{6}$$

More abstract version of 1st Friedmann equation is

$$\Big(\frac{1}{H_0}\frac{da/dt}{a}\Big)^2 = \Omega_{r,0}\Big(\frac{1}{a^4}\Big) + \Omega_{m,0}\Big(\frac{1}{a^3}\Big) + \Omega_{k,0}\Big(\frac{1}{a^2}\Big) + \Omega_{\Lambda,0} \tag{7}$$

In radiation dominated universe ($x = \frac{m_\chi}{T}$)
We have the energy density

$$\rho = \sum_i \rho_i = \frac{\pi^2}{30} g_*(T) T^4 \tag{8}$$

$$H(x) = \frac{H(m_\chi)}{x^2} \tag{9}$$

where

$$H(m_\chi) = \sqrt{\frac{\pi^2}{90}\frac{g_*(T)}{{M_{pl}}^2}{m_\chi}^4} \tag{10}$$

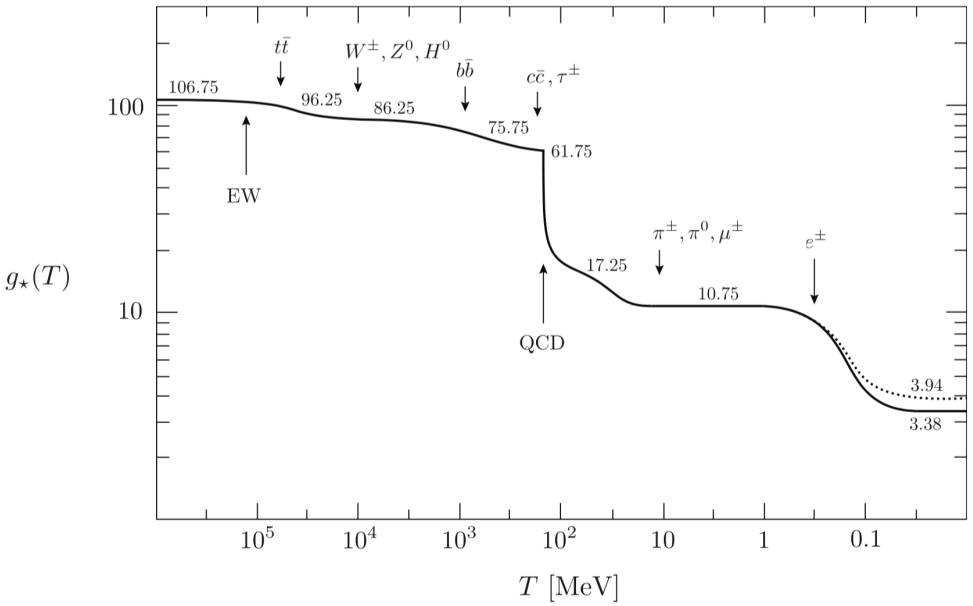

Figure 1: The change of effective massless degree of freedom $g_*(T)$ in terms of temperature T in radiation dominant universe(For standard model $SU(3) \otimes SU(2) \otimes U(1)$). Solid line is $g_*(T)$ and doted line is $g_{*S}(T)$. (From D.Baumann's cosmology note [7])

For the entropy S, we can also have [1] [7]

$$S(T) = \frac{2\pi^2}{45} g_{*,S}(T) T^3 \tag{11}$$

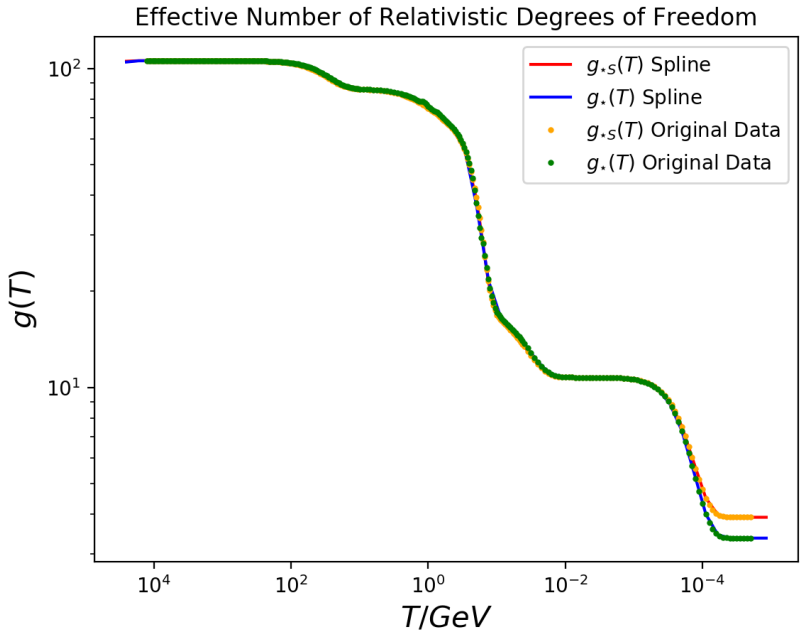

Figure 2: We input the numerical value of $g(T)$ in the scheme of Standard Model $SU(3) \otimes SU(2) \otimes U(1)$. We also use the Spline to do the interpolation.

So we can have that

$$S(x) = \frac{2\pi^2}{45} g_{*S}(T) {m_\chi}^3 \frac{1}{x^3} \tag{12}$$

Number density in arbitrary distribution

$$n_i(T) = n(T; m_i) = \int \frac{d^3\vec{k}}{(2\pi)^3} \frac{1}{\exp\left(-\frac{\sqrt{k^2+{m_i}^2}-\mu_i}{T}\right) + \eta_i} \tag{13}$$

(Boltzmann $\eta = 0$, Bose-Einstein $\eta = -1$, Fermi-Dirac $\eta = +1$).

In non-relativistic limit $\sqrt{k^2 + {m_i}^2} \approx m_i + \frac{k^2}{2m_i}$, and in low temperature limit we have $exp((E_i - \mu_i)/T) \gg 1$. n_i will follow Boltzmann distribution(Non-relativistic limit)

$$n_i(T) = g_i \left(\frac{m_i T}{2\pi}\right)^{3/2} exp\left(\frac{-(m_i - \mu_i)}{T}\right) \tag{14}$$

Integrable Boltzmann equation for $1 + 2 \leftrightarrow 3 + 4$

$$\frac{dn_1}{dt} + 3Hn_1 = \frac{dn_2}{dt} + 3Hn_2 = -\langle\sigma_{12\to34}v\rangle n_1 n_2 + \langle\sigma_{34\to12}v\rangle n_3 n_4 \tag{15}$$

$$\frac{dn_3}{dt} + 3Hn_3 = \frac{dn_4}{dt} + 3Hn_4 = -\langle\sigma_{34\to12}v\rangle n_3 n_4 + \langle\sigma_{12\to34}v\rangle n_1 n_2 \tag{16}$$

So we have (Don't need detailed balance)

$$\frac{dY_1}{dx} = \frac{dY_2}{dx} = -\frac{dY_3}{dx} = -\frac{dY_4}{dx} \tag{17}$$

Detailed balance for $1 + 2 \leftrightarrow 3 + 4$ for integrable Boltzmann equation

$$\langle \sigma_{12\to 34} \rangle n_1^{(eq)} n_2^{(eq)} = \langle \sigma_{34\to 12} \rangle n_3^{(eq)} n_4^{(eq)} \tag{18}$$

3 Boltzmann equation

3.1 Boltzmann Equation in FLRW (Isotropic&Homogeneous)

The general form of Boltzmann equation is

$$\frac{1}{E} L[f_\chi] = \frac{1}{E} C[f_\chi] \tag{19}$$

where the Liouville operator L in FLRW metric behaves like

$$\frac{1}{E} L = \frac{\partial}{\partial t} - \frac{\dot{a}(t)}{a(t)} \frac{|\vec{p}|^2}{E} \frac{\partial}{\partial E} \tag{20}$$

In relativistic situation, we have $E = \sqrt{p^2 + m_\chi^2}$. Using $EdE = pdp$ we have that

$$(\frac{\partial}{\partial t} - Hp\frac{\partial}{\partial p}) f_\chi(p, t) = \frac{1}{E} C[f_\chi] \tag{21}$$

where $p_\chi^\mu = (E, \vec{p})$.

Here we use the definition $p := |\vec{p}|$ and we assume that the density in phase space doesn't depend on the direction of the momentum(Isotropic) $\vec{p}$ and the location $\vec{x}$ (Homogeneous) , which means $f(p^\mu, x^\mu) = f(p, t)$.

What we will calculate later is coscattering collision process

$$\chi(\vec{p}) + \phi(\vec{k}) \to \psi(\vec{p'}) + \phi(\vec{k'}) \tag{22}$$

in our calculation ϕ and ψ are in thermal equilibrium(We will use this to simplify the collision in later calculation), however χ is treated as out of equilibrium.

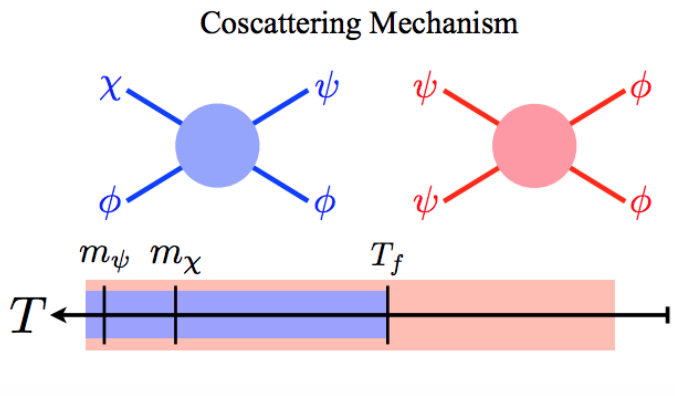

Figure 3: The mechanism of coscattering process and coannihilation process [2]. Here the blue Feynman diagram is related to the coscattering process $\chi + \phi \to \psi + \phi$. And the red Feynman diagram is related to the coannihilation process $\psi + \psi \to \phi + \phi$ (Since the process $\chi + \chi \to \phi + \phi$ and $\chi + \psi \to \phi + \phi$ is negligible, we don't plot their Feynmann diagram.). The mass of darkmatter particle χ is smaller than particle ψ(What is ψ, is it SM particle?).

3.2 Liouville Term Simplification

To simplify the Liouville term, we do the change of variable using dimensionless quantity

$$x(t) = \frac{m_\chi}{T(t)} \qquad (Time) \tag{23}$$

$$q(t,p) = \frac{p}{T(t)} \qquad (Momentum) \tag{24}$$

We will also make use of the definition of Hubble parameter $H(t) = \frac{\dot{a}(t)}{a(t)}$ and the change of radiation temperature in terms of scale parameter, which is $T(t) \propto \frac{1}{a(t)}$. So we will have that

$$\frac{1}{E}L = \frac{\partial}{\partial t} - H\vec{p}\cdot\frac{\partial}{\partial \vec{p}} = H\big(t(x)\big)x\frac{\partial}{\partial x} \tag{25}$$

3.3 Collision Term Simplification

The collision term is

$$\begin{aligned} C[f_\chi] = \frac{1}{2}\int d\Omega_{\vec{k}} d\Omega_{\vec{k}'} d\Omega_{\vec{p}'} (2\pi)^4 \delta^{(4)}(p + k - p' - k') |\overline{\mathcal{M}(\chi + \phi \leftrightarrow \psi + \phi)}|^2 \\ \times \Big[f_\phi(k',t) f_\psi(p',t) - f_\phi(k,t) f_\chi(p,t) \Big] \end{aligned} \tag{26}$$

where $d\Omega_{\vec{p}} = \frac{d^3\vec{p}}{(2\pi)^3 2E(p)}$ is the Lorentz invariant phase space.

We can define the velocity-averaged cross section(Invariant under Lorentz Transformation), which is

$$\langle\sigma v\rangle(s) = \int d\Omega_{\vec{p'}} d\Omega_{\vec{k'}} (2\pi)^4 \delta^{(4)}(p + k - p' - k') \frac{1}{2E(k)} \frac{1}{2E(p)} |\mathcal{M}|^2 \tag{27}$$

Because as we have mentioned before, ϕ and ψ are in thermal equilibrium($T << E_X$), we have that

$$f_X^{(eq)}(p,t) = \frac{1}{exp(\frac{E_{X,\vec{p}}}{T}) + 1} \approx exp(-\frac{\sqrt{|\vec{p}|^2 + m_X^2}}{T}) = exp(-\sqrt{(m_X/m_\chi)^2 q^2 + x^2}) \tag{28}$$

where $X = \phi, \psi, \chi$. Here χ is not in thermal equilibrium but we need $f_\chi^{(eq)}$ when using formula $f_\phi^{(eq)}(k',t) f_\psi^{(eq)}(p',t) = f_\phi^{(eq)}(k,t) f_\chi^{(eq)}(p,t)$ later.

So we have that

$$\frac{1}{E(p)} C[f_\chi] = \int \frac{d^3\vec{k}}{(2\pi)^3} \langle\sigma v\rangle(s) \Big[f_\phi(k',t) f_\psi(p',t) - f_\phi(k,t) f_\chi(p,t) \Big] \tag{29}$$

$$= \int \frac{d^3\vec{k}}{(2\pi)^3} \langle\sigma v\rangle(s) \Big[f_\phi^{(eq)}(k',t) f_\psi^{(eq)}(p',t) - f_\phi^{(eq)}(k,t) f_\chi(p,t) \Big] \tag{30}$$

$$= \int \frac{d^3\vec{k}}{(2\pi)^3} \langle\sigma v\rangle(s) \Big[f_\phi^{(eq)}(k,t) f_\chi^{(eq)}(p,t) - f_\phi^{(eq)}(k,t) f_\chi(p,t) \Big] \tag{31}$$

$$= \Big[f_\chi^{(eq)}(p,t) - f_\chi(p,t) \Big] \int \frac{d^3\vec{k}}{(2\pi)^3} \langle\sigma v\rangle(s) f_\phi^{(eq)}(k,t) \tag{32}$$

Here s is one of the Mandelstam variable, which is $s = (k+p)^2$.
Here we define that

$$C(p,t) = \int \frac{d^3\vec{k}}{(2\pi)^3} \langle\sigma v\rangle(s) f_\phi^{(eq)}(k,t) \tag{33}$$

So we have that

$$C[f_\chi] = \Big[f_\chi^{(eq)}(p,t) - f_\chi(p,t) \Big] C(p,t) \tag{34}$$

After combing the Liouville term and collision term together, we have that

$$H(x) x \frac{\partial f_\chi(x,q)}{\partial x} = \Big[exp(-\sqrt{x^2 + q^2}) - f_\chi(x,q) \Big] C(x,q) \tag{35}$$

Here $C(x,q)$ is a 3D integration so I plan to use Monte-Carlo method to do the integration.
After getting $f_\chi(x,q)$ numerically, we can calculate the related number density n_χ, which is

$$n_\chi\big(T(t)\big) = \int \frac{d^3\vec{p}}{(2\pi)^3} f_\chi(p,T) = T^3 \int \frac{d^3\vec{q}}{(2\pi)^3} f_\chi(q,x) = \Big(\frac{m_\chi}{x}\Big)^3 \int \frac{d^3\vec{q}}{(2\pi)^3} f_\chi(q,x) \tag{36}$$

3.4 $\langle\sigma v\rangle$ calculation

Let's follow the calculation of [4] and [5] and extend the consequence to more general case $m_1 \neq m_2$.

In cosmic comoving frame, where gas is assumed to be at rest as a whole part, we have

$$\langle\sigma v\rangle = \frac{\int \sigma v_{Mol} e^{-E_1/T} e^{-E_2/T} d^3\vec{p_1} d^3\vec{p_2}}{\int e^{-E_1/T} e^{-E_2/T} d^3\vec{p_1} d^3\vec{p_2}} \tag{37}$$

Here $v_{Mol} = \sqrt{|\vec{v_1} - \vec{v_2}|^2 + |\vec{v_1} \times \vec{v_2}|^2}$. Even though v_{Mol} itself is not invariant under Lorentz transformation, we can prove that $v_{Mol} E_1 E_2$ is invariant under Lorentz transformation. Let's prove it:

$$\begin{aligned} F(\tilde{s}) &= \sqrt{(p_1^\mu p_{\mu_2})^2 - {m_1}^2 {m_2}^2} \\ &= \frac{\sqrt{\tilde{s}^2 - 2({m_1}^2 + {m_2}^2)\tilde{s} + (m_1^2 - m_2^2)^2}}{2} \end{aligned} \tag{38}$$

Finally, we can show that

$$v_{Mol} = \frac{F(\tilde{s})}{E_1 E_2} \tag{39}$$

The distribution function is $f(E) = e^{-E/T}$, which is Maxwell-Boltzmann distribution.

Let's simplify $d^3\vec{p_1} d^3\vec{p_2}$.

If function $f = f(\theta_{12}, |\vec{v_1}|, |\vec{v_2}|)$ only depends on the angle θ_{12} between $\vec{p_1}$ and $\vec{p_2}$, $|\vec{p_1}|$ and $|\vec{p_2}|$, we will have that

$$\begin{aligned} &\int d^3\vec{p_1} d^3\vec{p_2} \quad y(\theta_{12}, p_1, p_2) \\ &= \int {p_1}^2 dp_1 dcos\theta_1 d\phi_1 \int {p_2}^2 dp_2 dcos\theta_{12} d\phi_{12} \quad y(\theta_{12}, p_1, p_2) \\ &= \int (4\pi)^2 p_1 E_1 dE_1 p_2 E_2 dE_2 \frac{1}{2} dcos\theta_{12} \quad y(\theta_{12}, p_1, p_2) \end{aligned} \tag{40}$$

We do the replacement of variable, which is

$$E_\pm = E_1 \pm E_2 \tag{41}$$

$$\tilde{s} = (p_1^\mu + p_2^\mu)^2 = ({m_1}^2 + {m_2}^2) + 2E_1 E_2 - 2p_1 p_2 cos\theta_{12} \tag{42}$$

Here we can know the range of e

So we have that

$$\begin{aligned} &\int 2\pi^2 E_1 E_2 dE_+ dE_- d\tilde{s} \quad y(\theta_{12}, p_1, p_2) \\ &= \int 2\pi^2 E_1 E_2 \frac{\partial(E_+, E_-, \tilde{s})}{\partial(E_1, E_2, cos\theta_{12})} dE_1 dE_2 dcos\theta_{12} \quad y(\theta_{12}, p_1, p_2) \\ &= \int (4\pi)^2 p_1 E_1 dE_1 p_2 E_2 dE_2 \frac{1}{2} dcos\theta_{12} \quad y(\theta_{12}, p_1, p_2) \end{aligned} \tag{43}$$

So we have that for $y(\theta_{12}, p_1, p_2)$,

$$d^3\vec{p}_1 d^3\vec{p}_2 = 2\pi^2 E_1 E_2 dE_+ dE_- d\tilde{s} \tag{44}$$

When $\frac{p_1}{p_2} = \frac{m_1}{m_2}$ and $cos\theta_{12} = 1$, we can get its minimum of $\tilde{s}$

$$\tilde{s}_{min} = (m_1 + m_2)^2 \tag{45}$$

We can have the range

$$|E_-| \leq \sqrt{1 - \frac{2({m_1}^2 + {m_2}^2)}{\tilde{s}}}\sqrt{{E_+}^2 - \tilde{s}} \tag{46}$$

$$E_+ \geq \sqrt{\tilde{s}} \tag{47}$$

$$\tilde{s} \geq 2({m_1}^2 + {m_2}^2) \tag{48}$$

The integration representation of Modified Bessel Function we will use later is(See [8])

$$K_n(x) = \frac{\sqrt{\pi}(x/2)^n}{\Gamma(n + \frac{1}{2})} \int_0^{+\infty} dt \quad \sinh t^{2n} \exp(-\cosh tx) \tag{49}$$

$$K_n(x) = \int_0^{+\infty} dt \quad \cosh nt \exp(-\cosh tx) \tag{50}$$

So we can have the integration

$$\begin{aligned}
&\int \sigma v_{Mol} e^{-E_1/T} e^{-E_2/T} d^3\vec{p}_1 d^3\vec{p}_2 \\
&= 2\pi^2 \int_{\tilde{s}=2({m_1}^2+{m_2}^2)}^{+\infty} d\tilde{s} \quad \sigma(\tilde{s}) F(\tilde{s}) \int_{E_+=\sqrt{\tilde{s}}}^{+\infty} e^{-E_+/T} dE_+ \int_{E_-=-\sqrt{1-\frac{2({m_1}^2+{m_2}^2)}{\tilde{s}}}\sqrt{{E_+}^2-\tilde{s}}}^{E_-=+\sqrt{1-\frac{2({m_1}^2+{m_2}^2)}{\tilde{s}}}\sqrt{{E_+}^2-\tilde{s}}} dE_- \\
&= 4\pi^2 \int_{\tilde{s}=2({m_1}^2+{m_2}^2)}^{+\infty} d\tilde{s} \quad \sigma(\tilde{s}) F(\tilde{s}) \sqrt{1 - \frac{2({m_1}^2 + {m_2}^2)}{\tilde{s}}} \int_{E_+=\sqrt{s}}^{+\infty} dE_+ e^{-E_+/T} \sqrt{{E_+}^2 - \tilde{s}} \\
&= 4\pi^2 T \int_{\tilde{s}=2({m_1}^2+{m_2}^2)}^{+\infty} d\tilde{s} \quad \sigma(\tilde{s}) F(\tilde{s}) \sqrt{\tilde{s} - 2({m_1}^2 + {m_2}^2)} K_1(\frac{\sqrt{\tilde{s}}}{T})
\end{aligned} \tag{51}$$

and

$$\int e^{-E_{1,2}/T} d^3\vec{p}_{1,2} \tag{52}$$

$$= 4\pi \int_{E_{1,2}=m_{1,2}}^{+\infty} \exp(-E_{1,2}/T) \sqrt{{E_{1,2}}^2 - {m_{1,2}}^2} E_{1,2} dE_{1,2} \tag{53}$$

$$= 4\pi (m_{1,2})^2 T K_0(\frac{m_{1,2}}{T}) \tag{54}$$

Finally we have

$$\langle \sigma v_{Mol} \rangle = \frac{\int_{\tilde{s}=2({m_1}^2+{m_2}^2)}^{\tilde{s}=+\infty} d\tilde{s} \quad \sigma(\tilde{s}) F(\tilde{s}) \sqrt{\tilde{s} - 2({m_1}^2 + {m_2}^2)} K_1(\frac{\sqrt{\tilde{s}}}{T})}{4T\Big({m_1}^2 K_0(\frac{m_1}{T})\Big)\Big({m_2}^2 K_0(\frac{m_2}{T})\Big)} \tag{55}$$

3.5 Compare with integrable Boltzmann equation

After the calculation using non-integrable Boltzmann equation, we can calculate it using integrable integrable version(To get integrable version, we need to do some approximation on its collision term $\int \frac{d^3\vec{p}}{(2\pi)^3} C[f_\chi]$.

Since we have the detailed balance

$$\langle \sigma_{\chi\to\psi} v\rangle n_\chi^{(eq)} = \langle \sigma_{\psi\to\chi}\rangle n_\psi^{(eq)} \tag{56}$$

$$\langle \sigma_{\psi\psi\to\phi\phi}\rangle n_\psi^{(eq)} n_\psi^{(eq)} = \langle \sigma_{\phi\phi\to\psi\psi}\rangle n_\phi^{(eq)} n_\phi^{(eq)} \tag{57}$$

So we can have the equation(Assuming that $n_\psi = n_\psi^{(eq)}$ and $n_\phi = n_\phi^{(eq)}$)

$$\frac{dn_i}{dt} + 3Hn_i = -\sum_j \left[n_\phi^{(eq)} \langle \sigma_{i\to j} v\rangle \left(n_i - n_i^{(eq)} \frac{n_j}{n_j^{(eq)}}\right) + \langle \sigma_{ij} v\rangle \left(n_i n_j - n_i^{(eq)} n_j^{(eq)}\right)\right] \tag{58}$$

The first term is related to the coannihilation process $\chi + \phi \to \psi + \phi$ and its inverse process $\psi + \phi \to \chi + \phi$. The second term is related to the coscattering process $\psi + \psi \to \phi + \phi$, $\chi + \psi \to \phi + \phi$(Negligible) and $\chi + \psi \to \phi + \phi$(Negligible). The index i, j can be chosen as $i, j = \chi, \psi$.

Assuming that we can have that

$$\frac{dn_\chi}{dt} + 3Hn_\chi = -n_\phi^{(eq)} \langle \sigma_{\chi\to\psi} v\rangle \left(n_\chi - n_\chi^{(eq)}\right) \tag{59}$$

$$\frac{dn_\psi}{dt} + 3Hn_\psi = -n_\phi^{(eq)} n_\psi^{(eq)} \langle \sigma_{\psi\to\chi} v\rangle \left(1 - \frac{n_\chi}{n_\chi^{(eq)}}\right) \tag{60}$$

We define that

$$Y_i = \frac{n_i}{S} \tag{61}$$

Since we have that

$$\frac{d}{dt} = H(x) x \frac{d}{dx} \tag{62}$$

$$\frac{dS}{dt} + 3H(x)S(x) = 0 \tag{63}$$

So we have that

$$\frac{dn_i}{dt} + 3H(x)n_i = SH(x)x\frac{d}{dx} \tag{64}$$

So in radiation dominated universe

$$\frac{dY_\chi}{dx} = -\frac{S(x)}{H(x)x} \langle \sigma_{\chi\to\psi} v\rangle Y_\phi^{(eq)} Y_\chi^{(eq)} \left(\frac{Y_\chi}{Y_\chi^{(eq)}} - 1\right) \tag{65}$$

Here let's derive $H(m_\chi)$. We already have the Friedmann equation (6) which is $H^2 = \frac{1}{3{M_{pl}}^2}\rho$ (Here $k \approx 0$). For the radiation dominant universe, we have

$$H(x) = \frac{H(m_\chi)}{x^2} \tag{66}$$

$$S(x) = \frac{S(m_\chi)}{x^3} \tag{67}$$

where

$$H(m_\chi) = \sqrt{\frac{\pi^2}{90}\frac{g_*(T)}{{M_{pl}}^2}{m_\chi}^4} \tag{68}$$

$$S(m_\chi) = \frac{2\pi^2}{45} g_{*S}(T) {m_\chi}^3 \tag{69}$$

Don't forget that $x = \frac{m_\chi}{T}$.

This equation can be solved using adaptive RK4(Not stable), Crank-Nicolson(More stable, but still not enough), Backward Euler(Very stable). I will mainly use Backward Euler in later calculation.

We will compare (35) (36) and (60) to see the difference between these two approaches. My another goal is to reproduce the consequences in Joshua's paper [2].

4 Numerical Calculation

4.1 Equation to solve

From [2], we know the example dark sector(Toy model) is

$$\mathcal{L} \supset -\frac{m_\chi}{2}\chi^2 - \frac{m_\psi}{2}\psi^2 - \delta m \chi\psi - \frac{y}{2}\phi\psi^2 + h.c. \tag{70}$$

$$\langle\sigma_{\chi\to\psi}v\rangle(x) = \left(\frac{m_\psi}{m_\chi}\right)^{\frac{3}{2}} e^{-\Delta x}\langle\sigma_{\psi\to\chi}v\rangle \tag{71}$$

$$\approx \left(\frac{m_\psi}{m_\chi}\right)^{\frac{3}{2}} e^{-\Delta x} f(r)\sqrt{\Delta}\frac{y^4\delta^2}{2\pi m_\chi^2} \tag{72}$$

where

$$f(r) = \frac{(r^2+r+2)^2}{\sqrt{2}(r-2)^2 r^{9/2}(r+1)^{7/2}} \tag{73}$$

Also here we use the dimensionless quantity to represent the m_ϕ and m_ψ.

$$r = \frac{m_\phi}{m_\chi} \tag{74}$$

$$\Delta = \frac{m_\psi - m_\chi}{m_\chi} \tag{75}$$

After some algebra, we have the ODE

$$\frac{dY_\chi}{dx} = -\frac{45^{3/2}}{2^{7/2}\pi^8}\frac{1}{g_{\star S}(m_\chi/x)\sqrt{g_\star(m_\chi/x)}}\left(f(r)(1+\Delta)^{3/2}\Delta^{1/2}y^4\delta^2\right)\left(\frac{M_{pl}}{m_\chi}\right)\left(\frac{e^{-\Delta x}}{x^2}\right) \\ \times I_b^{(eq)}(x, R=r)I_b^{(eq)}(x, R=1)\left(\frac{Y_\chi}{Y_\chi^{(eq)}} - 1\right) \tag{76}$$

Here

$$I_b^{(eq)}(x, R) = \int_0^{+\infty} d\xi \frac{\xi^2}{\exp\left(\sqrt{\xi^2 + (Rx)^2}\right) - 1} \tag{77}$$

and

$$Y_i^{(eq)}(x) = \frac{45}{4\pi^4 \cdot g_{\star S}(m_\chi/x)} I_b^{(eq)}(x, R = \frac{m_i}{m_\chi}) \tag{78}$$

4.2 Some tricky treatment for doing integration

There is some trick thing on the calculation of $I_b^{(eq)}(x, R)$ when using Python. It will be very easy to meet the situation when the calculation overflows. When $x \leq 20$, we can set the do such operation:

$$I_b^{(eq)}(x, R) = \int_0^{+\Lambda} d\xi \frac{\xi^2}{\exp\left(\sqrt{\xi^2 + (Rx)^2}\right) - 1} \tag{79}$$

Here we choose $\Lambda = 700$(If $\Lambda > 700$ the numerical consequence of $I_b^{(eq)}(x, R)$ will diverge.). When $x > 20$, since $\frac{1}{e^{20}} \sim 10^{-9}$, so we can do the approximation

$$I_b^{(eq)})(x, R) \approx \int_0^{+\infty} d\xi \frac{\xi^2}{\exp\left(\sqrt{\xi^2 + (Rx)^2}\right)} = (Rx)^2 K_2(Rx) \tag{80}$$

So we technically we make the $I_b^{(eq)}(x, R)$ to be

$$I_b^{(eq)}(x, R) = \begin{cases} \int_0^{+\Lambda} d\xi \frac{\xi^2}{\exp\left(\sqrt{\xi^2 + (Rx)^2}\right) - 1} & 0 \leq Rx < 20 \\ (Rx)^2 K_2(Rx) & Rx \geq 20 \end{cases} \tag{81}$$

Let's compare different method for the calculation of $I_b^{(eq)}(x, R)$, the first method is (81). The second one is using python recommend "integrate.quad" to calculate $I_b^{(eq),2}(x, R) = \int_0^\infty d\xi \frac{\xi^2}{\exp\left(\sqrt{\xi^2+(Rx)^2}\right)-1}$ by brutal force. We compare the numerical consequence of these

two method and compare it with the consequence of Mathematica(15 digits at least)(See Figure 4). We can find blue line(81) behaves much better than green line(brutal force), so we will use the formula (81) to do later calculation.

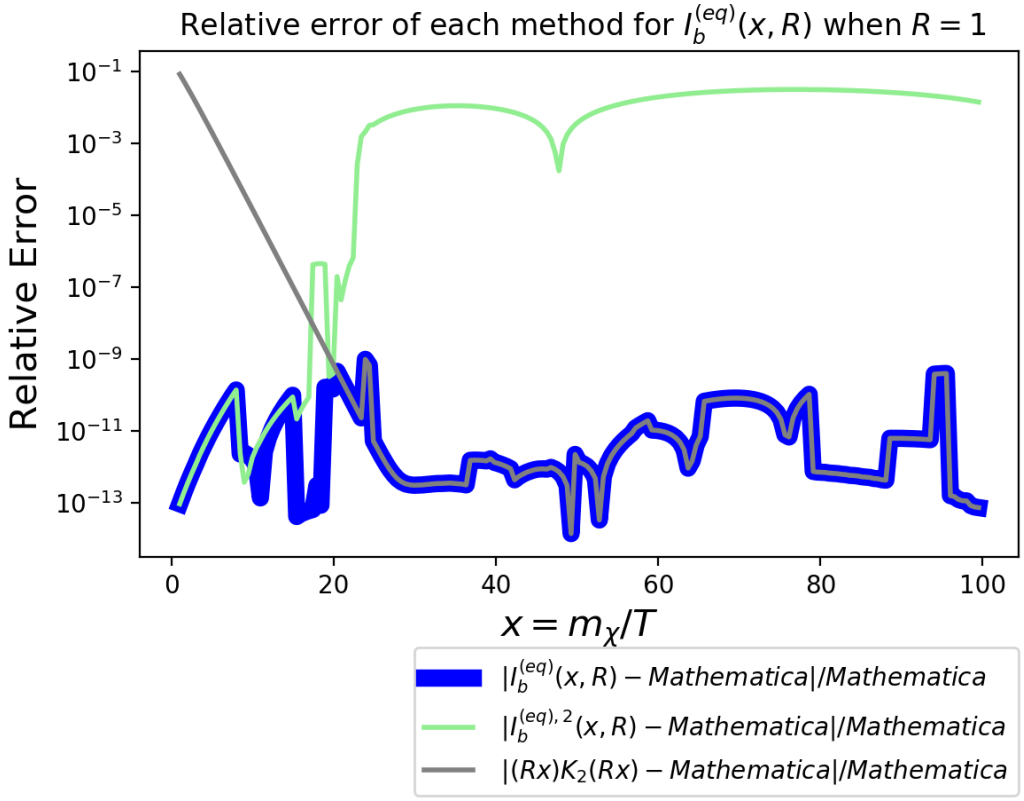

Figure 4: Here the green line is related to the brutal force calculation of $\int_0^\infty d\xi \quad \xi^2/\left[\exp\left(\sqrt{\xi^2+(Rx)^2}\right)-1\right]$ using python. The blue line is our choosed method which calculate $\int_0^\Lambda d\xi \quad \xi^2/\left[\exp\left(\sqrt{\xi^2+(Rx)^2}\right)-1\right]$ when $Rx < 20$(Here we choose $\Lambda = 700$). When $Rx \geq 20$, the whole integration tends to become much more like Boltzmann integration, so we omit -1 and get analytical approximation $RxK_2(Rx)$. We comepare these two consequence with the consequence from Mathematica(as bench mark). We can find blue line behaves much better and $Relative \quad error \sim 10^{-9}$, however the green line behavies badly, when $Rx \geq 20$, $Relative \quad error \sim 10^{-1}$. However the region $Rx \geq 20$ still should be considered so it is not wise to use brutal force calculation(green line).

4.3 Change parameter $r = m_\phi/m_\chi$

Here we varies the $r = m_\phi/m_\chi$ to see its influence on the process of freezing out of dark matter χ.

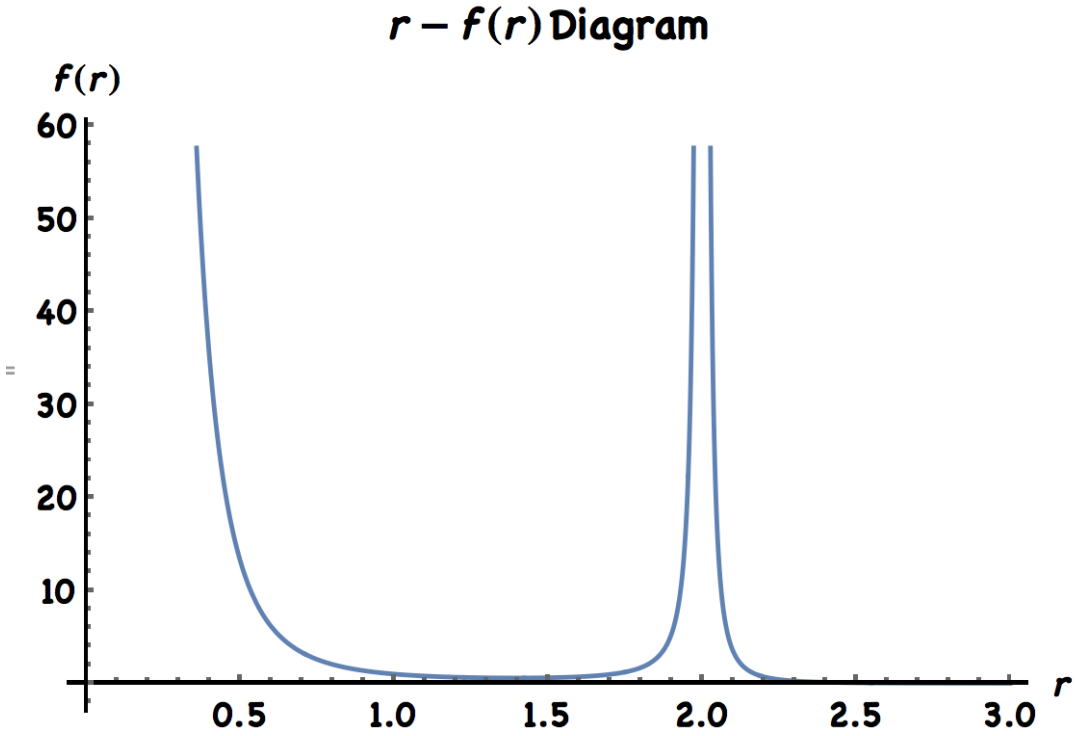

Figure 5: Don't forget $f(r) = \frac{(r^2+r+2)^2}{\sqrt{2}(r-2)^2 r^{9/2}(r+1)^{7/2}}$. In Josh's paper,only region $0 < r \leq 1$ are considered. In this region $(0 < r \leq 1)$, $f(r)$ decreases when r increases.

We can see that when r becomes larger and smaller than 1, $f(r)$ decreases, which is related to the decreasing of collision term. The decreasing of collision means that DM interactes weaker with thermal bath so when the RHS term (collision) of Boltzmann equation decreases, the DM χ will freeze out earlier(smaller $x_{Freeze-out}$).

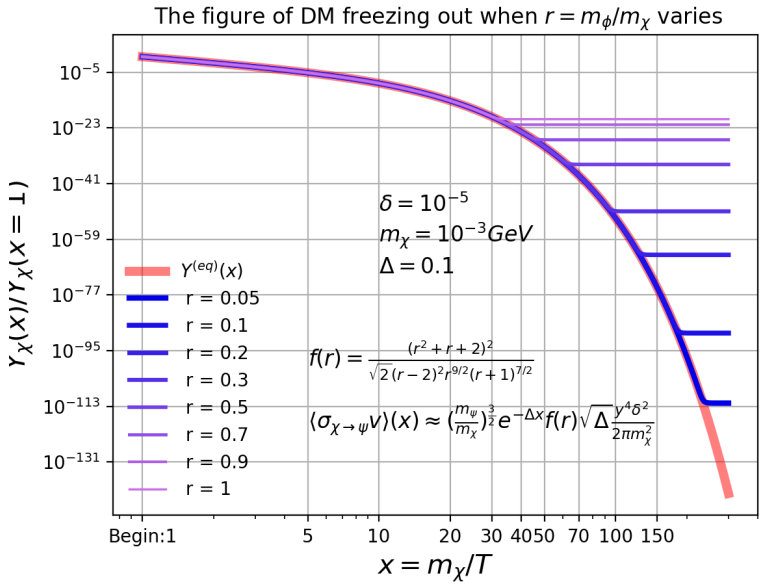

Figure 6: Parameter set 1 (See figure): This is $x - Y_\chi$ diagram for different $r = m_\phi/m_\chi$. When $0 < r \leq 1$ increases, χ will freeze out earlier.

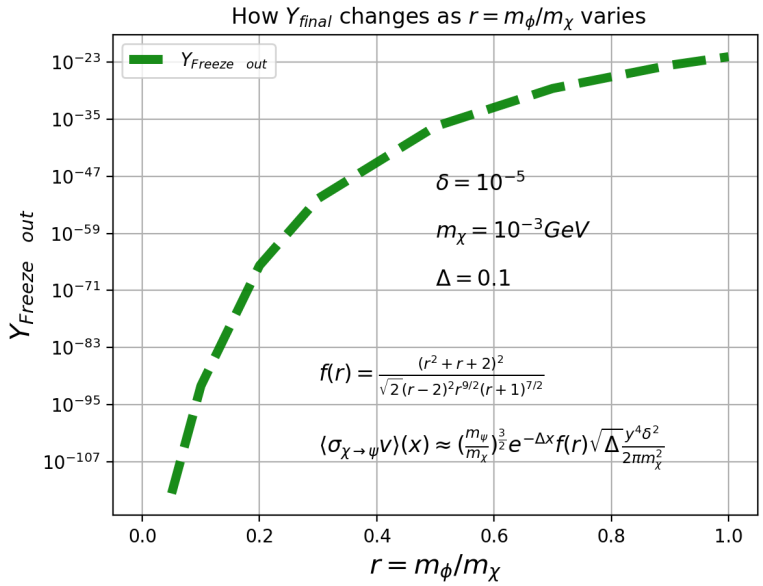

Figure 7: Parameter set 1 (See figure): This is the plot of $r - Y_{Freeze-out}$. There is one thing inconsistent with Josh's consequence: when $r \to 0$, $Y_{Freeze-out}$ should tends to a constant. However, in my calculation, when $r \to 0$, $Y_{Freeze-out}$ is still decreasing. I guess the reason is that $f(r)$ we use is only the approximation and $f(r) \to \infty$ when $r \to 0$. In exact $f(r)$ form, there might be some factor to suppress the divergence of $f(r)$(I need to figure this out later).

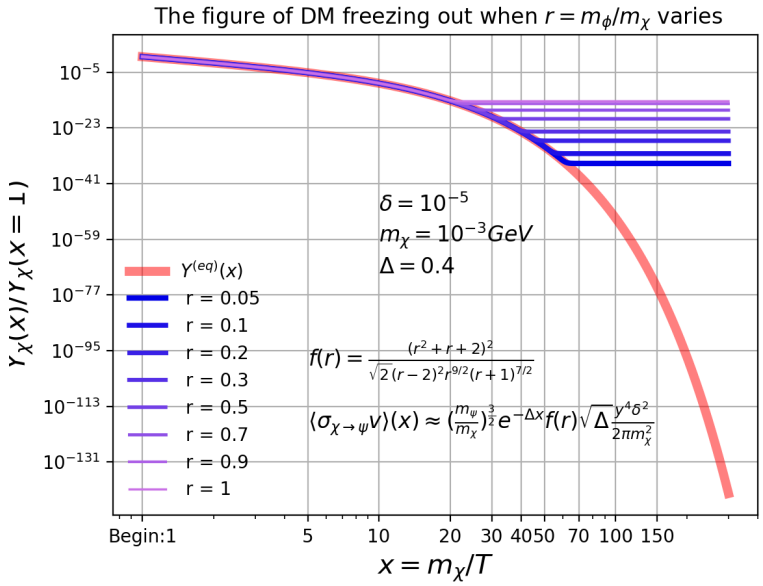

Figure 8: Parameter set 2 (See figure): This is $x - Y_\chi$ diagram for different $r = m_\phi/m_\chi$. When $0 < r \leq 1$ increases, χ will freeze out earlier. We can see that the tail of freezing out is more dense comparing with Figure 6. This is caused by the larger $\Delta(\Delta = 0.4 > 0.1)$.

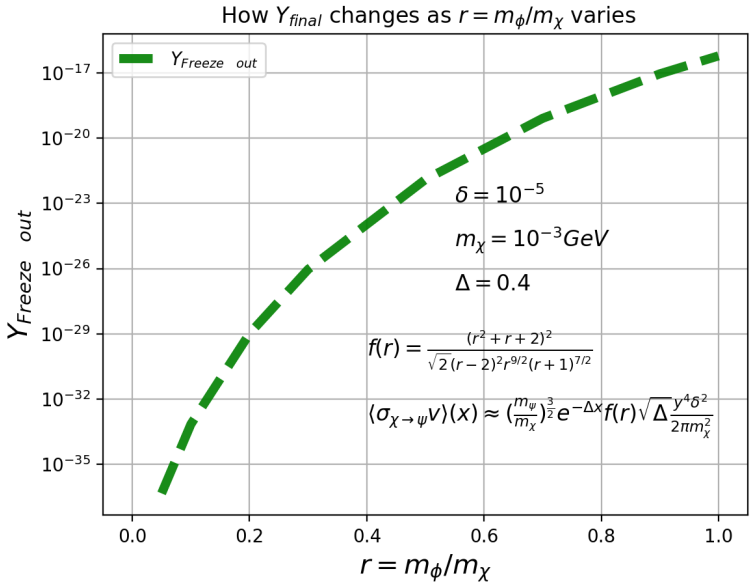

Figure 9: Parameter set 2 (See figure): This is the plot of $r - Y_{Freeze-out}$. There is also the similar thing inconsistent with Josh's consequence.

4.4 Change parameter $\Delta = (m_\psi - m_\chi)/m_\chi$

Here we can see the change of $Y_{Freeze-out}$ in terms of Δ is not monotonic(This is not consistent with Josh's consequence). The reason is because of the approximation of the calculation, the factor $\Delta^{1/2}\Delta^{3/2}e^{-x\Delta}$ is not monotonic. When $\Delta \to 1$ or $\Delta \to 0$, definitely the collision term will decrease, so the coupling of χ with thermal bath will become weaker(This means DM χ will decouple earlier). However, when $\Delta \sim 0.01 - 0.1$, the coupling of χ with thermal bath might be stronger, which makes χ decouples later.

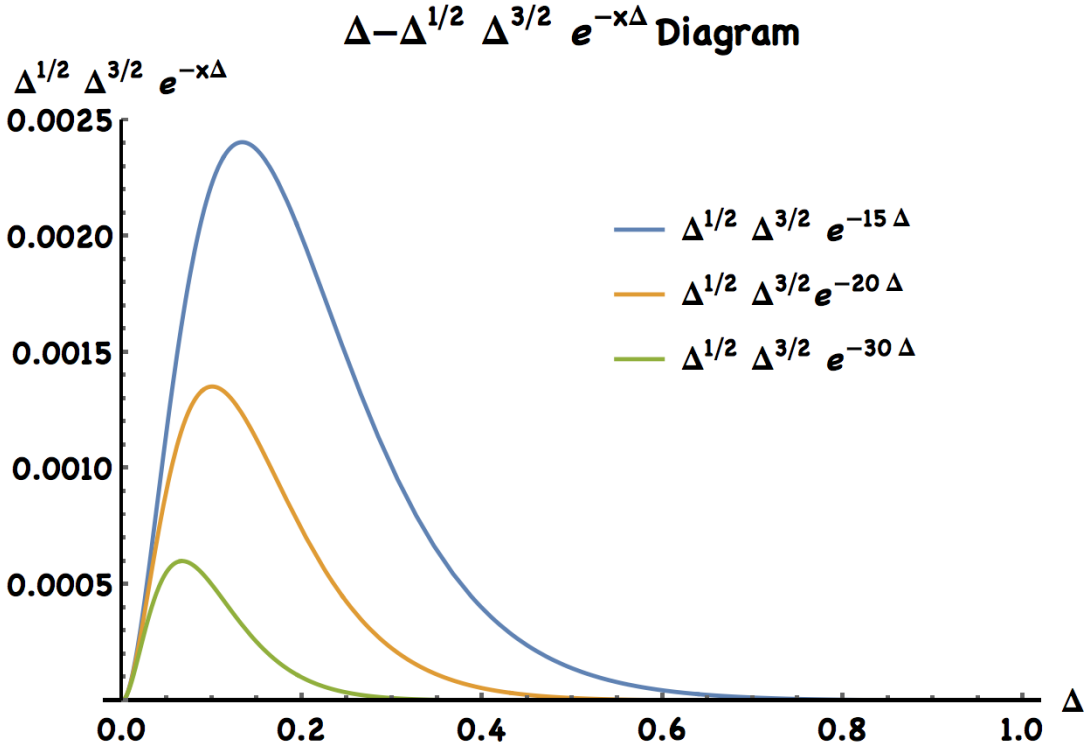

Figure 10: The part in collision term which will vary with Δ is $\Delta^{1/2}\Delta^{3/2}e^{-x\Delta}$. We can see that function $\Delta^{1/2}\Delta^{3/2}e^{-x\Delta}$ is not a monotonic function of Δ. When $x \sim 20$, the peak is around 0.1.

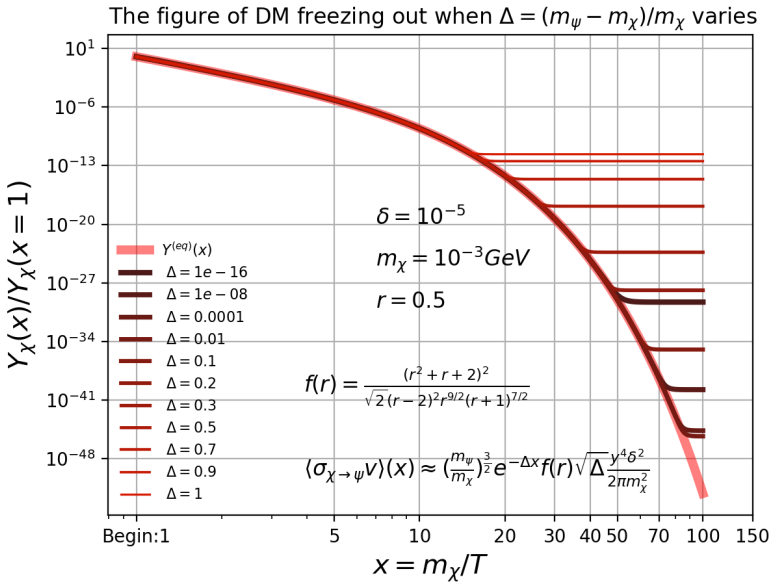

Figure 11: Parameter set 3 (See figure): This is $x - Y_\chi$ diagram for different $\Delta = (m_\psi - m_\chi)/m_\chi$. We can find that when $\Delta \sim 0.01$, the coupling of χ and thermal bath becomes maximum. When $\Delta \leq 0.01$ or $\Delta \geq 0.01$, the coupling begins to decrease.

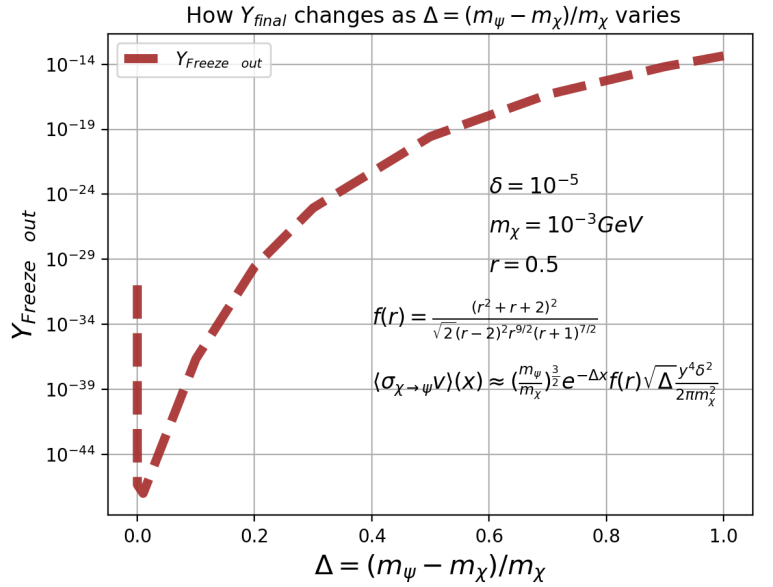

Figure 12: Parameter set 3 (See figure): This is the plot of $\Delta - Y_{Freeze-out}$. From this diagram, we can draw similar conclusion as Figure 11

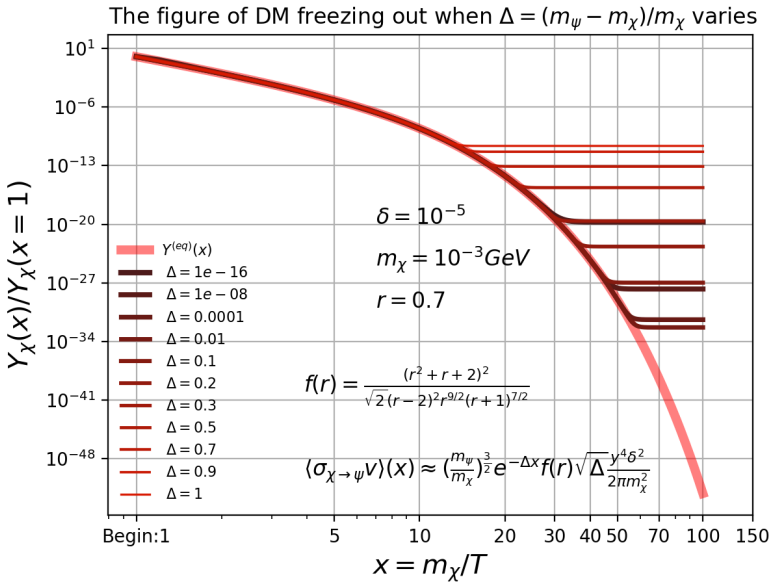

Figure 13: Parameter set 4 (See figure): This is $x - Y_\chi$ diagram for different $\Delta = (m_\psi - m_\chi)/m_\chi$. Also, we can draw similar conclusion as Figure 11. Another thing should be noted is that comparing with Figure 11, we can find the final $Y_{Freeze-out}$ is more dense, the reason is that larger r ($r = 0.7 > 0.5$) will lift the $Y_{Freeze-out}$ apparently.

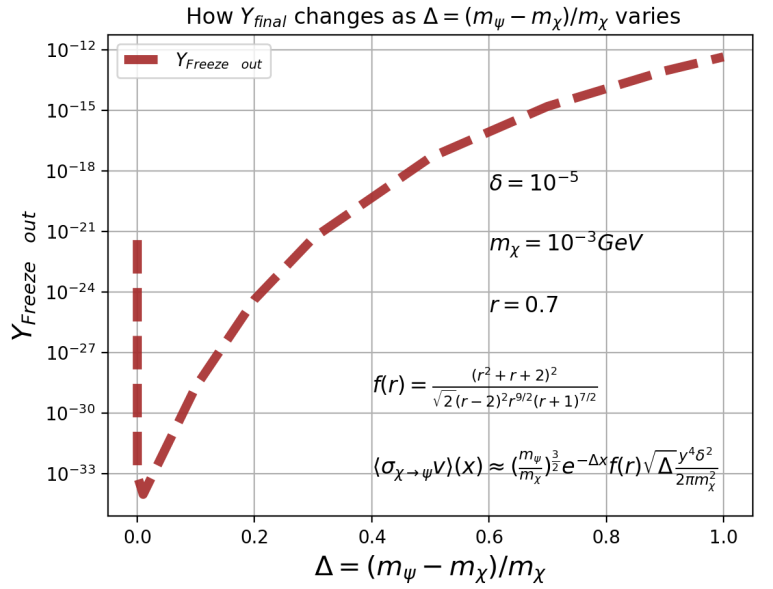

Figure 14: Parameter set 4 (See figure): This is the plot of $\Delta - Y_{Freeze-out}$. We can draw similar conclusio as above diagrams.

5 Self-Consistency check

One of the most important thing of numerical calculation is self-consistency check. We vary the parameter only will appear in the numerical calculation rather than real physics situation to see whether the numerical consequences(Physical consequences) are related to these irrelevant parameters. If not sensitive, we will be confident to believe(Still not make sure) that our numerical method is correct. Here we vary iteration steps N_t and initial x_0 to see how sensitive the consequence(Here is $X_{Freeze-out}$ and $Y_{Freeze-out}$) depends on them.

Fortunately, the physics consequences are not sensitive on N_t and x_0 and the error is of $1\% - 3\%$ scale(When $N_t \geq 5000$) when N_t changes and of $0.1\% - 1\%$ when x_0 changes. For DM freeze out research(Which we mostly care about $log(Y)$), this precision is already good enough.

5.1 Change time step number N_t

Table 1: Change of $Y_{Freeze-out}$ when N_t changes

N_t	50	70	100	200
$Y_{Freeze-out}$	10.003×10^{-37}	5.915×10^{-37}	4.079×10^{-37}	2.712×10^{-37}
N_t	1000	5000	10000	50000
$Y_{Freeze-out}$	1.996×10^{-37}	1.882×10^{-37}	1.868×10^{-37}	1.857×10^{-37}

* $r = 0.5$, $\Delta = 0.1$, $m_\chi = 10^{-3} GeV$, $x_0 = 1$

We change the iteration step number N_t from 50 to 50000. In Figure 15 we can find that these lines overlap with each other. So if we only want to draw the diagram of DM freezing out, even $N_t = 50$ is enough. From Table 1, we can see that quantitatively, when $N_t \geq 5000$, the relative error is only 3$ and this as acceptable.

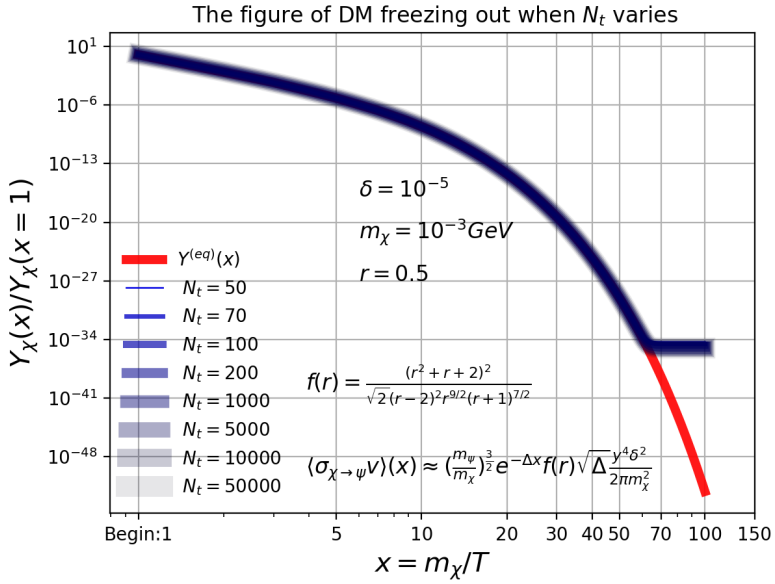

Figure 15: Parameter set 1: Self consistency check when N_t changes. This is $x - Y_\chi$ diagram.

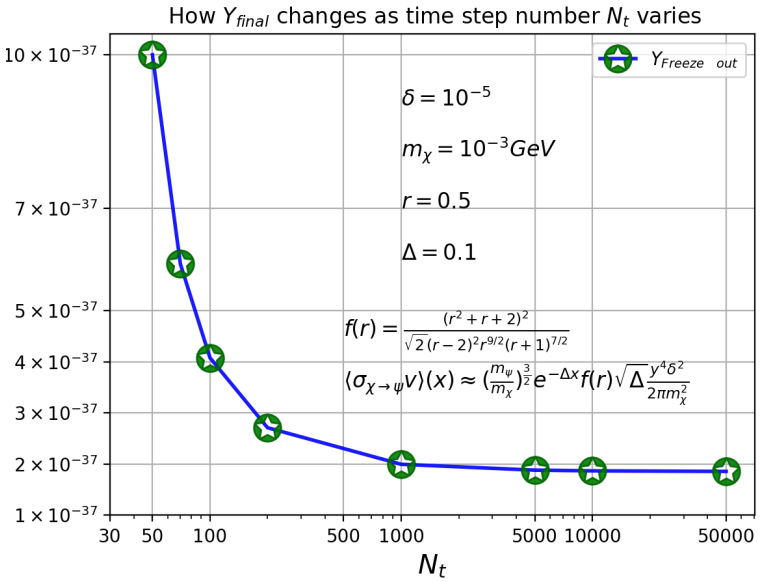

Figure 16: Parameter set 1: Self consistency check when N_t changes. This is $N_t - Y_{Freeze-out}$ diagram. We can see that when $N_t \geq 5000$, the error of the consequence is already small enough.

5.2 Change initial x_0

Table 2: The relative error of $Y_{Freeze-out}$ when x_0 changes

x_0	0.1	1	5	10
Relative Error	0×10^{-4}	1.34×10^{-4}	7.31×10^{-4}	1.48×10^{-3}
x_0	15	20	25	30
Relative Error	2.22×10^{-3}	2.96×10^{-3}	3.71×10^{-3}	4.45×10^{-3}
x_0	35	40	45	50
Relative Error	5.19×10^{-3}	5.93×10^{-3}	6.67×10^{-3}	7.41×10^{-3}

* $r = 0.5$, $\Delta = 0.1$, $m_\chi = 10^{-3}GeV$, $N_t = 5000$ ($\sim 2\%$precision, good enough)
** Relative Error:$= (Y_{Freeze-out}(x_0) - Y_{Freeze-out}(0.1))/Y_{Freeze-out}(0.1)$

Here we change the initial x_0, we find that the relative error is only around 0.1% so this is acceptable.

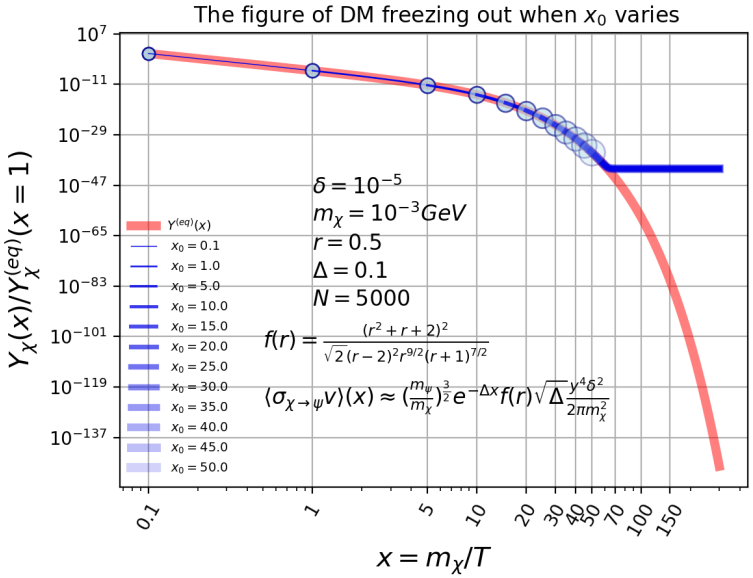

Figure 17: Parameter set 1: Thicker the line, larger the x_0 is. The circle label where the DM evolution begins and its also similar, larger the circle, larger the x_0 is.

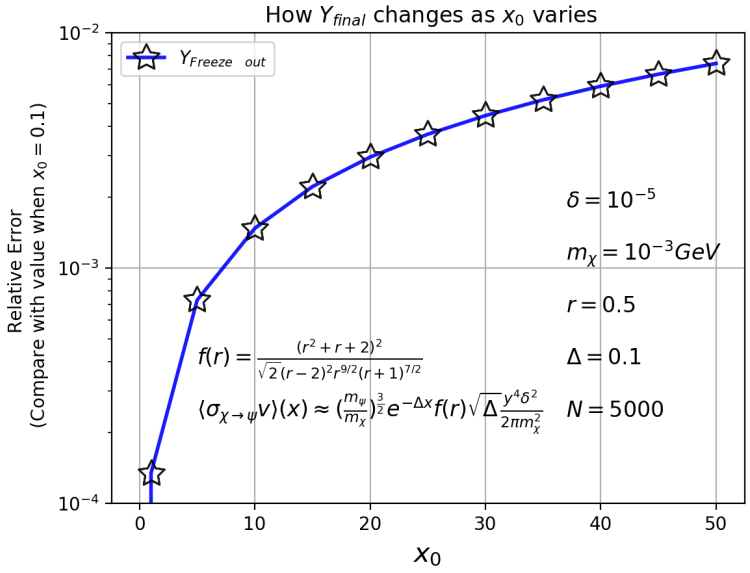

Figure 18: Parameter set 1: x_0-Relative error diagram. Here we can see the relative error is only around 0.1%, so the numerical consequence is not sensitive with the changing of x_0.

6 Appendix A: WIMP Miracle

It seems I have no time to deal with famous WIMP miracle, I will do it in the future.

7 Future Goal

1. Consider more series model rather than the toy model shown in this final paper.(Care about how $f(r)$ and other terms behaves when $r \to 1$ and $\Delta \to 1$)
2. Apply higher order implicit method(For example, implicit RK) to do the calculation.
3. Solve non-integrable Boltzmann equation and compare with integrable Boltzmann equation.

References

[1] Kolb, Edward. The early universe. CRC Press, 2018.

[2] DAgnolo, Raffaele Tito, Duccio Pappadopulo, and Joshua T. Ruderman. "Fourth Exception in the Calculation of Relic Abundances." Physical review letters 119, no. 6 (2017): 061102.

[3] Garny, Mathias, Jan Heisig, Benedikt Llf, and Stefan Vogl. "Coannihilation without chemical equilibrium." Physical Review D 96, no. 10 (2017): 103521.

[4] Lisanti, Mariangela. "Lectures on dark matter physics." In New Frontiers in Fields and Strings: TASI 2015 Proceedings of the 2015 Theoretical Advanced Study Institute in Elementary Particle Physics, pp. 399-446. 2017.

[5] Gondolo, Paolo, and Graciela Gelmini. "Cosmic abundances of stable particles: Improved analysis." Nuclear Physics B 360, no. 1 (1991): 145-179.

[6] Cannoni, Mirco. "Lorentz invariant relative velocity and relativistic binary collisions." International Journal of Modern Physics A 32, no. 02n03 (2017): 1730002.

[7] Baumann, Daniel. "Cosmology, part III mathematical tripos." University lecture notes (2014).

[8] NIST, Integration formulas of Modified Bessel Functions, https://dlmf.nist.gov/10.32

[9] https://en.wikipedia.org/wiki/Friedmann_equations